Origin of Magnetic Circular Dichroism in GaMnAs: Giant Zeeman Splitting versus Spin Dependent Density of States

M. Berciu,[1] R. Chakarvorty,[2] Y. Y. Zhou,[2] M. T. Alam,[3] K. Traudt,[2] R. Jakiela,[4] A. Barcz,[4] T. Wojtowicz,[4] X. Liu,[2] J. K. Furdyna,[2] and M. Dobrowolska[2,*]

[1]*Department of Physics and Astronomy, University of British Columbia, Vancouver, BC, V6T 1Z1, Canada*
[2]*Department of Physics, University of Notre Dame, Notre Dame, Indiana 46556, USA*
[3]*Department of Electrical Engineering, University of Notre Dame, Notre Dame, Indiana 46556, USA*
[4]*Institute of Physics, Polish Academy of Sciences, 02-668 Warsaw, Poland*
(Received 19 January 2009; published 18 June 2009)

We present a unified interpretation of experimentally observed magnetic circular dichroism (MCD) in the ferromagnetic semiconductor (Ga,Mn)As, based on theoretical arguments, which demonstrates that MCD in this material arises primarily from a difference in the density of spin-up and spin-down states in the valence band brought about by the presence of the Mn impurity band, rather than being primarily due to the Zeeman splitting of electronic states.

Although a multitude of magneto-optical (MO) studies have attempted to elucidate the effect of magnetism occurring in GaMnAs (both in the epilayer and quantum well forms) on its band properties, their results are conflicting [1–12]. So far the interpretation of the MO data in GaMnAs was carried out using a model similar to that used successfully for II-Mn-VI diluted magnetic semiconductors (DMSs), based on the presence of strong interactions between magnetic moments and electronic bands via *s, p-d* exchange, that leads to a giant Zeeman splitting of electronic states [13]. Various MO experiments on II-VI DMSs yielded a consistent picture of this exchange mechanism [13]. In particular, it was found that the *p-d* exchange constant β (now known with relatively high precision) has antiferromagnetic (AFM) character in all II-VI DMSs, due to virtual transitions between the *p* and the half filled 3*d* orbitals.

The same approach, when used to analyze MO data in GaMnAs, results not only in a wide range of values for β [2,4,12] but, more importantly, in conflicting reports about its sign [ferromagnetic (FM) or AFM] [6,9,12], raising questions about the exchange process between Mn moments and band carriers. The correct interpretation of this process is of fundamental importance, since it has major consequences for our understanding of the effect of magnetism occurring in any III-Mn-V system on its band properties, and therefore for possible future applications. The most commonly used technique to study MO properties of GaMnAs is magnetic circular dichroism (MCD), which arises from magnetic-field-induced differences in the absorption of right and left circularly polarized light, and is given by the expression

$$\mathrm{MCD} = \frac{T^+ - T^-}{T^+ + T^-} \propto \frac{(\alpha^- - \alpha^+)d}{2}. \qquad (1)$$

Here T^+ and T^- are transmission intensities for σ^+ and σ^- circular polarizations (which connect the spin-down

and spin-up holes with the conduction band (CB) states, respectively), and $\alpha^\pm$ are the corresponding absorption coefficients. When the difference between α^+ and α^- near the band gap is caused by a Zeeman shift, the polarity of the MCD signal identifies the sign of the *p-d* exchange constant. However, the shape and polarity of the MCD spectrum in GaMnAs is observed to depend on growth conditions [2,7], resulting sometimes in only positive MCD signal, and sometimes in both negative and positive parts. Application of the Zeeman shift model then leads to a FM (positive MCD) or AFM (negative MCD) sign for β, explaining the contradictory claims in the literature.

However, Zeeman shift is not the only mechanism of MCD. It can also arise due to magnetic-field-induced population changes and/or mixing of states (see, e.g., Ref. [14]). In this Letter we present a unified interpretation of experimental MCD data, supported by theoretical arguments, which demonstrates that MCD in GaMnAs arises primarily from a difference in the density of spin-up and spin-down states in the valence band (VB), brought about by the presence of the Mn impurity band (IB), rather than being primarily due to a Zeeman shift.

GaMnAs samples with thickness of 0.3 μm were grown by molecular beam epitaxy on (001) GaAs substrates. Samples with Mn concentration $x \approx 0.01$ were grown on a 0.4 μm thick ZnSe buffer, while samples with $x = 0.0003$ and 0.002 were grown on a 0.2 μm $Ga_{0.70}Al_{0.30}As$ buffer. Both buffers serve as excellent etch stops, which allowed us to etch away the GaAs substrate in order to eliminate its contribution to optical transmission. The Mn (and Be, when appropriate) concentrations were determined by secondary ion mass spectrometry, showing a very uniform Mn distribution throughout the layers. The Curie temperatures for samples exhibiting FM behavior were obtained from SQUID magnetization data. The MCD measurements were performed in

the transmission mode using polarization modulation via a photoelastic modulator.

Figure 1(a) shows MCD spectra for a $Ga_{0.984}Mn_{0.016}As$ sample taken in a magnetic field of 5.0 T at temperatures $T = 1.7, 20, 40,$ and 70 K, i.e., from well below to well above its Curie temperature T_C of 26 K. The MCD spectra show a broad positive signal, which rises sharply in the vicinity of the energy gap, has a peak around 1.6–1.7 eV, and extends well beyond the band gap. Similar MCD spectra were observed on FM samples by several other authors [1,6,7]. As T increases, the magnitude of MCD decreases steadily, while the energy at which the sharp rise occurs remains unchanged. This behavior is drastically different from that observed in II-VI DMSs. As an example, Fig. 1(b) shows the MCD spectra for $Cd_{0.963}Mn_{0.037}Te$ taken at similar values of B and T. Here the MCD shows a negative peak (a consequence of AFM character of the p-d exchange constant) centered at the energy gap. As T increases, the spectrum narrows as both its onset and its termination energies shift, reflecting a strong temperature dependence of the s, p-d enhanced giant Zeeman splitting of the band edges [13]. The drastic differences in the shape and temperature dependence of the MCD spectra of these two materials suggests that they likely result from different mechanisms.

The fundamental difference between II-Mn-VI and III-Mn-V systems lies in the fact that the divalent Mn acts as an acceptor in the III-V host. Compared to Ga^{3+} ions, Mn^{2+} creates a much weaker Coulomb attraction for VB electrons. Taking the host's background as reference, this results in an effective repulsive potential near the Mn site, pushing one eigenstate above the VB, thus forming an impurity state near the Mn ion, while the valence band is depleted by one state. Normally this state would be empty (i.e., filled by a hole). However, in a compensated sample this state can be filled by an electron from a donor, such as As_{Ga}. Since Mn^{2+} is magnetic, the energy of this state is determined not only by the effective repulsion, but also by the AFM p-d exchange which contributes a fair amount to the total "binding" energy [15]. This leads to AFM correlations between the spin of Mn^{2+} and of the hole (FM correlations with the electron, in compensated samples) occupying the impurity level. Consequently, there is one fewer electron state with spin oriented parallel to the Mn spin left in the valence band.

We will now discuss the MCD spectrum of a sample with a low Mn concentration x, where the impurity levels have broadened into an IB. For that purpose we calculated, using the standard Kubo formula [16], the α^+ and α^- absorption spectra using a one-dimensional (1D) "toy model." The VB and CB were modeled by nearest neighbor hopping on two sublattices, with hopping integrals chosen to give reasonable effective masses and an on-site potential on one sublattice chosen to give a gap of 1.5 eV. Mn^{2+} ions were assumed to be randomly distributed on sites of the VB sublattice. For simplicity, we assumed them to be fully spin polarized by an applied magnetic field, and chose their impurity potential and AFM p-d exchange with VB electrons so as to give a binding energy of 0.1 eV. The results shown in Fig. 2 are for a system with $N = 500$ sites per sublattice and 10 Mn ($x = 0.02$). The oscillatory behavior seen at higher energies is a result of finite-size effects in the density of states (DOS). Minimizing this effect requires large N and is the reason why 3D calculations, which involve full diagonalization of matrices of linear dimension $\sim N^3$, are effectively impossible.

Figure 2(a) shows $\alpha^{\pm}$ absorption spectra and the resulting MCD signal for a sample with an empty IB (no com-
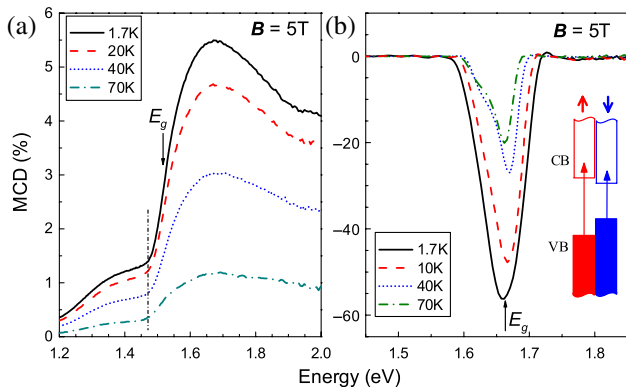

FIG. 1 (color online).   (a) MCD spectra taken at $B = 5.0$ T and $T = 1.7, 20, 40,$ and 70 K on a $Ga_{0.984}Mn_{0.016}As$ layer grown at 280 °C. The dash-dotted vertical line marks the onset of the sharp rise of MCD. (b) MCD spectra taken at 5.0 T for similar temperatures on a $Cd_{1-x}Mn_xTe$ sample with $x = 0.037$. The inset shows a schematic illustration of the spin split valence and conduction bands in CdMnTe, together with spin conserving transitions allowed for σ^+ and σ^- circular polarizations (right and left arrows, respectively).
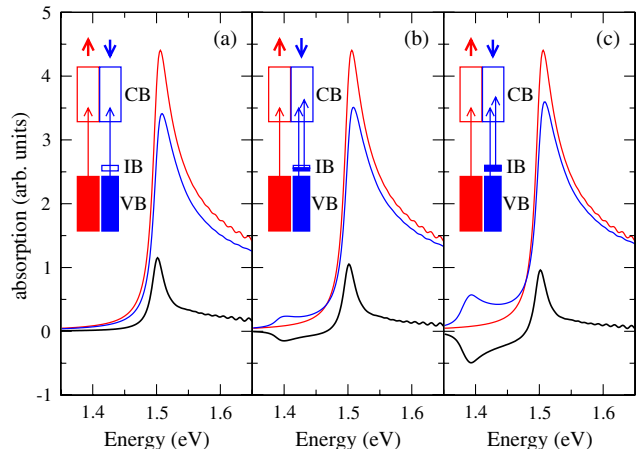

FIG. 2 (color online).   MCD signal (lowest line), α^- (topmost line), and α^+ (middle line) calculated for a 1D doped system which is (a) uncompensated, (b) partially compensated, and (c) fully compensated. The corresponding allowed transitions are shown schematically in the insets. The sharp peaks seen at E_g reflect the 1D density of states (DOS) which diverge at the band edges.

pensation). As sketched in the inset, contributions to $\alpha^{\pm}$ come only from VB → CB transitions, both starting at the band gap energy $E_g = 1.5$ eV. Assuming that the Mn spins are fully polarized by the applied magnetic field, there are $1 - x$ times fewer spin-down states than spin-up states in the VB, and consequently α^+ absorption is weaker than α^- absorption. This spin dependent difference in the DOS of the VB leads to a positive MCD signal (black line in the figure), which rises sharply at the energy gap. If the system is partially [Fig. 2(b)] or fully [Fig. 2(c)] compensated, transitions from IB to CB will also take place. However, since the impurity band states are now occupied by spin-down electrons, these transitions will contribute only to the α^+ absorption. Therefore the difference between the two absorptions due to IB-to-CB transitions will now result in a negative contribution to the MCD signal starting at an energy $E_g - \Delta_{BE}$ (where Δ_{BE} is the binding energy), i.e., about ~1.4 eV, and extending into higher energies. Above E_g the MCD signal will have two competing contributions for compensated samples: a positive contribution arising from the difference in the density of states in the VB (as discussed above) and a negative contribution due to IB-to-CB transitions. The resulting MCD signal will then depend on the degree of compensation, as well as on the matrix elements of the contributing transitions.

As discussed above, we used a simplified 1D model in our calculations. Since the 3D DOS vanishes at the band edges, one expects the MCD signal to peak at an energy higher than E_g, where the DOS in the VB is depleted the most by contributions to the IB. For a simple impurity wave function $\langle \vec{r}|I \rangle \sim \exp(-r/a_B)$, the contribution from VB states of momentum k is $p(k) \propto k^2|\langle \vec{k}|I \rangle|^2 \propto k^2(k^2 + 1/a_B^2)^{-2}$ (k^2 is due to phase-space volume). Contributions from heavy-hole (HH) states with energy $\epsilon_h(k) = \hbar^2 k^2/2m_h$ are then $p(\epsilon) = p(k)dk/d\epsilon \sim \sqrt{\epsilon}(2m_h\epsilon/\hbar^2 + 1/a_B^2)^{-2}$, with a maximum at $\epsilon_h = \hbar^2/(6m_h a_B^2)$. Since optical transitions conserve momentum, the maximum of the MCD signal due to the difference in DOS between the spin-up and spin-down states in the VB should then occur at an energy $E_{max} = E_g + \epsilon_h + \epsilon_e$ where $\epsilon_e = \hbar^2/(6m^* a_B^2)$, m^* being the CB effective mass. For light holes (LH) one gets a similar formula, but with the HH mass replaced by the LH mass in ϵ_h. Using typical values $a_B \sim 10$ Å, $m_h \sim 0.5m_e$, and $m_l \sim m^* \sim 0.07m_e$ gives $E_{max} \sim 1.71, 1.86$ eV for HH and LH, respectively. These very rough estimates are consistent with the MCD spectrum shown in Fig. 1(a) for a sample with very small degree of compensation. The above model explains not only the sign of the MCD signal and the energy range where it peaks, but also the temperature independence of the sharp jump in the positive contribution to MCD, as seen experimentally [see Fig. 1(a)]. According to our model this onset depends only on E_g, which is temperature independent in the range studied [17].

The most direct verification of the proposed scenario comes from measurements of α^+ and α^- at $B = 5$ T

shown in Fig. 3 for a GaMnAs film with $x = 0.0003$. The sample was grown at a temperature of 600 °C in order to minimize formation of As_{Ga} antisites. An antireflection coating was evaporated onto the sample surface to suppress Fabry-Perot oscillations for photon energies near the band gap. Examination of Fig. 3 indicates that the difference between the α^+ and α^- curves is mainly caused by a "vertical" rather than "horizontal" shift, suggesting that the difference between the two absorptions is dominated by the difference in the density of states involved in the spin-up and spin-down transitions, rather than by the Zeeman shift of the absorption edges.

We will now compare the predictions of the model with the MCD data shown in Fig. 4(a) for several GaMnAs films. Samples A, B, and D have the same Mn concentration $x = 0.014$, but were grown under different conditions, resulting in different levels of compensation: Sample D was grown at 200 °C, samples A and B were grown at 250 °C, and sample A was additionally codoped with Be. As a result, sample D is expected to be highly compensated, while sample A has the lowest degree of compensation. As our model predicts, the below-gap negative contribution to MCD signal is the strongest in sample D, still visible in sample B, but absent in sample A. Above the band gap the positive MCD signal for the highly compensated sample D is considerably weaker than for samples A and B. This again is consistent with our model, because the above-E_g MCD signal has two opposite contributions, and since in sample D the number of spin-down electrons occupying IB is roughly equal to the number of spin-up states depleted from the VB, the resulting signal should be significantly smaller than in samples with lower compensation.

We now consider the shape of the above-gap spectrum. Sample B provides clear evidence for the existence of two
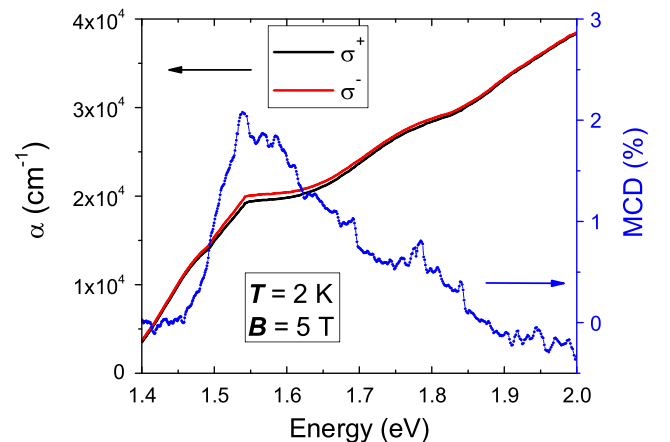

FIG. 3 (color online).   Absorption spectra of GaMnAs with $x = 0.0003$ taken at 5 T and $T = 2$ K for circular polarizations σ^+ and σ^-. The corresponding MCD calculated from the σ^+ and σ^- absorption curves as $(\alpha^- - \alpha^+)d/2$ is also plotted. The MCD is dominated by a single broad peak centered at 1.565 eV, corresponding to the energy range where $d\alpha/dE$ is negligible.
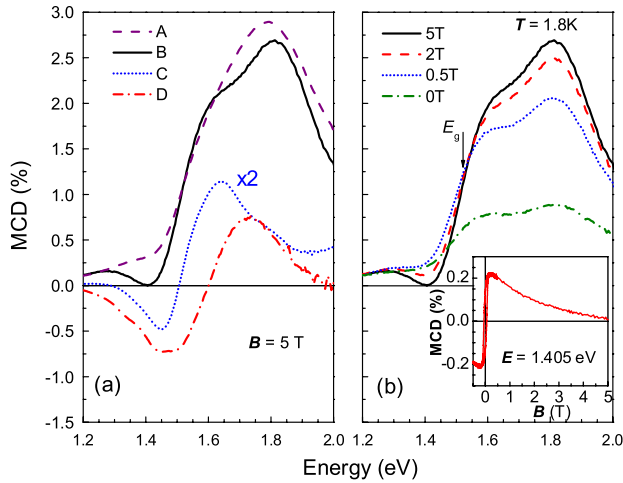
FIG. 4 (color online).   (a) MCD spectra taken at $T = 1.8$ K and $B = 5.0$ T for several GaMnAs samples. Samples A, B, and D have $x = 0.014$, while sample C has $x = 0.002$. For other details, see text. (b) MCD spectra taken on sample B at $T = 1.8$ K and $B = 0$, 0.5, 2, and 5 T. The horizontal line marks MCD $= 0$. Inset: Magnetic field dependence of MCD for sample B observed at $T = 1.8$ K at photon energy 1.405 eV, showing a small but finite hysteresis loop.

MCD peaks above E_g, at locations consistent with our rough estimates for HH and LH contributions. This identification is further supported by the presence of only one peak (at $\sim$1.65 eV) in sample C, grown at $T_S = 260\,°C$ with a much lower Mn concentration $x = 0.002$. Since in the single-impurity limit the largest contribution to the impurity state comes from heavy holes [15,16], we expect to see only the HH peak in the MCD signal for very low x, as indeed evidenced by sample C. However, as x increases and the HH states around the optimum energy become exhausted, one expects to see more of the LH states as well as states deeper in the VB being pulled into the IB. This is consistent with the emergence of the second peak (around 1.85 eV) in sample B, and the broad unresolved peak at $\sim$1.8 eV in sample A.

A final check of our scenario comes from the variation of MCD with changing magnetic field, shown in Fig. 4(b) for sample B. The FM character of this sample ($T_C = 16$ K) is evidenced by the presence of MCD signal at zero magnetic field, where, however, we only observe the positive part of MCD produced by interband transitions. The absence of the negative contribution at $B = 0$ indicates that, even though the sample is FM, the IB states filled by electrons are not spin polarized at $B = 0$. Only the empty (i.e., hole-occupied) states in the IB are spin polarized, thereby giving rise to a difference in the spin-up and spin-down DOS in the VB, and consequently to a positive MCD signal above E_g. This is fully consistent with the picture proposing that the Mn-Mn interaction in low-x samples is mediated by holes hopping inside an IB [18–21]. Only the Mn ions with high overlap with these holes can be ordered magnetically at T_C, and in turn polarize the spins of the holes weakly

bound to them. The Mn spins with low overlap with the holes, i.e., those with impurity states filled with electrons, remain paramagnetic down to very low temperatures. Since these Mn are not polarized, neither are the electrons filling the states bound to them.

When a magnetic field is applied, however, it polarizes these Mn spins and they in turn polarize their corresponding bound states, which results in a gradual emergence of IB-to-CB transitions, and thus in an onset of a negative contribution to MCD below E_g. This is precisely the behavior seen experimentally in Fig. 4(b). What follows then is that the negative part of MCD must mirror the paramagnetic behavior of the relevant Mn spins. This is verified in the inset of Fig. 4(b), which shows that the magnetic field dependence of the MCD signal measured at 1.4 eV follows a paramagnetic behavior, even though the hysteresis loop seen in the inset indicates a FM character of the sample as a whole.

In conclusion, this work explains in a unified manner the complex behavior of MCD in GaMnAs that has long been a puzzle in this field. The solution is drastically different from that based on the giant Zeeman shift relevant to II-Mn-VI DMS, and underscores again the importance of the impurity band to our understanding of III-Mn-V DMSs.

---

*mdobrowo@nd.edu

[1] B. Beschoten *et al.*, Phys. Rev. Lett. **83**, 3073 (1999).
[2] T. Hartmann *et al.*, Phys. Rev. B **70**, 233201 (2004).
[3] J. Szczytko *et al.*, Solid State Commun. **99**, 927 (1996).
[4] J. Szczytko *et al.*, Phys. Rev. B **59**, 12 935 (1999).
[5] J. Szczytko *et al.*, Phys. Rev. B **64**, 075306 (2001).
[6] K. Ando *et al.*, Phys. Rev. Lett. **100**, 067204 (2008).
[7] R. Chakarvorty *et al.*, Appl. Phys. Lett. **91**, 171118 (2007).
[8] W. Heimbrodt *et al.*, Physica (Amsterdam) **10E**, 175 (2001).
[9] R. Lang *et al.*, Phys. Rev. B **72**, 024430 (2005).
[10] T. Komori *et al.*, Phys. Rev. B **67**, 115203 (2003).
[11] M. Poggio *et al.*, Phys. Rev. B **72**, 235313 (2005).
[12] R. C. Myers *et al.*, Phys. Rev. Lett. **95**, 017204 (2005).
[13] J. K. Furdyna, J. Appl. Phys. **64**, R29 (1988).
[14] P. J. Stephens, J. Chem. Phys. **52**, 3489 (1970).
[15] A. K. Bhattacharjee and C. B. a la Guillaume, Solid State Commun. **113**, 17 (1999).
[16] G. D. Mahan, *Many Particle Physics* (Plenum, New York, 1981).
[17] E. Grilli *et al.*, Phys. Rev. B **45**, 1638 (1992).
[18] M. Berciu and R. N. Bhatt, Phys. Rev. Lett. **87**, 107203 (2001).
[19] A. Kaminski and S. Das Sarma, Phys. Rev. Lett. **88**, 247202 (2002).
[20] G. Alvarez, M. Mayr, and E. Dagotto, Phys. Rev. Lett. **89**, 277202 (2002).
[21] B. L. Shen *et al.*, Phys. Rev. Lett. **99**, 227205 (2007).